Integrated Optical, Wavelength Selective, Acoustically Tunable 2 × 2 Switches (Add–Drop Multiplexers) in LiNbO3

Frank Wehrmann, Christiane Harizi, Harald Herrmann, Ulrich Rust, *Student Member, IEEE*, Wolfgang Sohler, and Susanne Westenhöfer

Abstract—Fully packaged, polarization independent, integrated acoustooptic 2 × 2 switches have been developed which can be also used as add/drop multiplexers. The devices have been fabricated in X-cut Y-propagating LiNbO3 and can be operated at wavelengths around 1550 nm. They consist of passive polarization splitters and acoustooptic TE-TM converters with weighted coupling. A filter bandwidth of 2.0 nm and a tuning range of 130 nm have been obtained. The fiber-to-fiber insertion loss is <4.6 dB and a residual polarization dependence of 1.3 dB for bar-state and 0.1 dB for cross-state routing has been achieved.

I. INTRODUCTION

INTEGRATED acoustooptic circuits in LiNbO3 are attractive devices for WDM communication systems [1]–[3]. Acoustooptic filters [4], [5] and wavelength selective switches [6], [7] have been developed offering narrowband filtering ($\approx$2 nm FWHM), broad tuning ranges (>100 nm) and fast tuning/switching (<10 μs). A unique property of the devices is their capability of simultaneously filtering/switching several wavelengths.

For WDM communication systems tunable add–drop multiplexers are key components. For example, they can be used to add and drop one or more channels at distinct wavelengths from a ring network [8]. Furthermore, it is possible to use the devices for broadcasting which can be realized by dropping only a small, arbitrary fraction of power at each node of the transmission line. In WDM network nodes the devices also find application as wavelength selective 2 × 2 space switches.

Most of the acoustooptic filters/switches investigated so far use external polarising components [5], [9], [10]. If polarization splitters are integrated, simple, nonweighted acoustooptical mode converters have been used [6], [11]. Moreover, many investigations up to now have been performed as "optical bench experiments" without pigtailing and packaging the devices.

It was the objective of this work to develop fully integrated 2 × 2 switches/add–drop multiplexers in LiNbO3 with polarization splitters and advanced acoustooptical mode
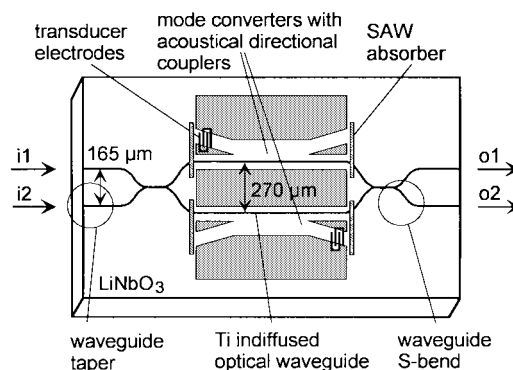
Fig. 1. Structure of the integrated optical 2 × 2 switch/add–drop multiplexer.

converters with weighted coupling [12] on a single substrate (see Fig. 1). Special attention has been paid to low insertion loss, low crosstalk and polarization insensitivity. Moreover, the devices have been fiber pigtailed and packaged allowing an easy handling and a reliable operation.

In the following section, we present the design of the switches/multiplexers and discuss their principle of operation. They are built by a combination of polarization splitters, bendings, and acoustooptical mode converters which are discussed in Section III. Results from investigations of the overall device will be given in Section IV.

II. SWITCH/MULTIPLEXER DESIGN AND PRINCIPLE OF OPERATION

The basic structure of the integrated optical switch is shown in Fig. 1. It consists of two polarization splitters/combiners and two acoustooptical mode converters. The incoming optical signal is split into two parts according to its polarization components by the first polarization splitter. TM polarized waves are routed to the bar-state, TE polarized waves to the cross-state output of the polarization splitter (Fig. 2). Assuming a signal entering at input port i1 the TM and TE components are directed toward the upper and lower mode converter, respectively (see Fig. 1). Within each mode converter the state of polarization (SOP) can be converted from TE to TM or vice versa. Behind the mode converters the two branches are recombined within a second polarization splitter being identical to the first one. If no mode conversion
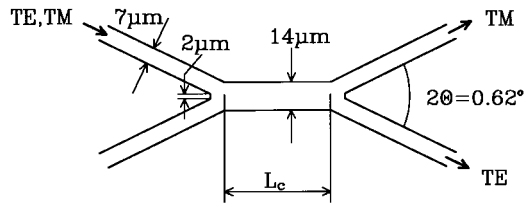
Fig. 2.   Design of the polarization splitters.

takes place, each polarization component of the input signal is passing both polarization splitters in the same manner (bar or cross). The input signal is, therefore, routed toward the output o1 of the device; the device is in the bar-state. If mode conversion takes place at the wavelength of the input signal, the TM (TE) polarized wave entering the upper (lower) mode converter is TE- (TM-) polarized when passing the second polarization splitter. Thus, the converted signal is routed toward output o2; the device is in the cross-state.

The mode conversion is accomplished via the interaction of the optical waves with a surface acoustic wave (SAW) being excited by applying a RF signal to the interdigital transducer electrodes. The acoustooptical mode conversion is a phase-matched process, i.e., the difference of the wavenumbers β_{TE} and β_{TM} of the fundamental TE- and TM-modes have to be equal to the wavenumber K_{ac} of the SAW:

$$\mid \beta_{\mathrm{TE}} - \beta_{\mathrm{TM}} \mid -K_{\mathrm{ac}} = 0. \tag{1}$$

$\Delta\beta = \beta_{\mathrm{TE}} - \beta_{\mathrm{TM}}$ is wavelength dependent which results in a strong wavelength selectivity of the acoustooptical mode conversion. Tuning is accomplished by varying K_{ac} via the SAW frequency f_{ac}.

By simultaneously applying several frequencies to the transducer electrodes, it is possible to switch several wavelengths at the same time.

As can be seen from Fig. 1, we use two separate mode converters with SAW's travelling into opposite directions to get identical frequency-shifts for TE- and TM-components. Otherwise, a beat signal will occur at twice the SAW frequency of ≈170 MHz if polarising elements are implemented between the cross-state output of the device and the optical receiver. This beating can reduce the performance of an optical network drastically. It should be noticed here that, to avoid the beating, both acoustooptical mode converters have to be operated at exactly the same frequency.

By adjusting the strength of the SAW via the RF drive power a maximum conversion efficiency of theoretically 100% can be achieved. Reducing the RF power results in lower conversion efficiencies so that the input signal is split and routed to both output ports (power tapping function).

III. COMPONENT DESIGN AND TECHNOLOGY

A. Optical Waveguides

The optical waveguides have been fabricated by an indiffusion of 7-μm-wide 100-nm-thick Ti-stripes. The diffusion has been performed at $T_D = 1060$ °C for 9 h. This process yields single-mode waveguides in the spectral range around $\lambda = 1550$ nm. Propagation losses are typically 0.1–0.2 dB/cm in both polarizations.

B. Polarization Splitters

The polarization splitters are based on two-mode interference in a directional coupler structure which is shown in Fig. 2. The structure has been slightly changed compared to the polarization splitters reported in [4] where the principle of operation is explained in more detail. The splitting ratio is defined as the ratio of the power in the unwanted output port and the total output power. With an opening angle of $2\Theta = 0.62°$ and central section lengths around $L_c = 300$ μm splitting ratios of more than 29 dB have been achieved with a single splitter for TE and TM polarized waves. As mentioned above each switch consists of two polarization splitters. It is not possible to measure the splitting ratio of each splitter separately as one had to cut the sample to do this. Therefore, all splitting ratios given in this paper have been obtained from the complete structure consisting of two splitters in series. These overall splitting ratios directly limit the extinction and therefore the inter-channel crosstalk in the cross-state output of the devices [11]. The two optical waveguides between the polarsation splitters form a Mach–Zehnder interferometer that might have a path difference between its arms due to fabrication tolerances. A nonzero path difference results in an improved splitting ratio of the total structure. Assuming two identical splitters and a path difference of zero, the splitting ratio of a single splitter is theoretically 6 dB better than that of the complete structure. Practically, the path difference is not known, so there is a residual uncertainty regarding the splitting ratio given above (29 dB for a single splitter).

It is not possible to obtain the excess losses of the splitters from the measured transmission ot the switch structure as they cannot be distinguished from the waveguide bending losses. In former investigations the excess losses of a polarization splitter have been measured to be 0.7 dB.

C. Waveguide Bendings

To allow fiber-chip coupling the two input and output branches are separated by 165 μm; in the converter sections the two optical waveguides are separated by 270 μm. Therefore, waveguide bendings are required. We use S-shaped circular arcs with a radius of 16 cm (see Fig. 3). An optical signal passing the device suffers losses from four bendings. The resulting total bending loss on a chip is ≪1 dB for TM and ≈1 dB for TE polarization.

D. Acoustooptical Mode Converters

The acoustooptical mode conversion is a wavelength-selective process resulting from the interaction of surface acoustic and optical waves. Using simple acoustooptical mode converters with a homogeneous coupling strength along the interaction length (i.e., constant SAW intensity at the location of the optical waveguide) the conversion efficiency as function of the optical wavelength shows sidelobes theoretically −9.7 dB below the maximum. A reduction of these sidelobes can
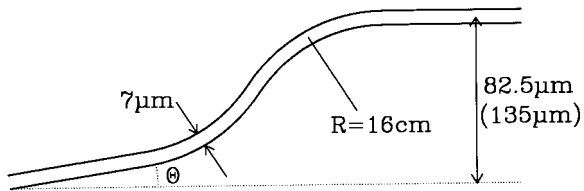
Fig. 3. Bending waveguide structure consisting of circular arcs ($R = 16$ cm). The lateral offset is 82.5 μm for bendings located between chip endface and polarization splitter and 135 μm for bendings located between polarization splitter and mode converter. 2Θ is the opening angle of the polarization splitter.
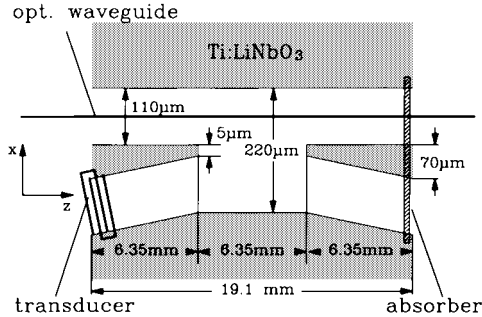

Fig. 4. Design of the acoustooptical mode converter with weighted coupling.

be achieved by cascading several mode converters [4], [13] or using different weighted coupling techniques [14]–[17].

The devices reported here use a tapered acoustical directional coupler structure (Fig. 4). With this structure, a sidelobe reduction down to about −22 dB is expected theoretically [12]. The acoustical waveguide stucture has been fabricated by Ti-indiffusion of 160-nm-thick Titanium layers into the cladding regions. The diffusion has been performed at 1060 °C for 24 h before the fabrication of the optical waveguides. The directional coupler is formed by 110-μm-wide acoustical waveguides. One of these guides is straight whereas the other one is inclined in the outer sections by an angle of 0.59° resulting in a linear change of the gap between 70 and 0 μm. To avoid sharp tips which are difficult to reproduce lithographically, the gap changes abruptly from 5 to 0 μm.

In the straight acoustical guide the optical waveguide is embedded; in the other arm the SAW is excited via an RF signal applied to the interdigital transducer electrode.

The acoustical directional coupler has been designed to yield a complete coupling cycle for the SAW, i.e., the acoustical power is coupled to the adjacent acoustical guide and back again. This results in a weighted acoustooptic interaction with a soft increase and cutoff of the acoustical intensity at the location of the optical waveguide. With such mode converters a sidelobe suppression down to about −20 dB has been achieved. A detailed analysis of the acoustooptical mode conversion within acoustical directional couplers is given in [12]. The SAW intensity distribution in the acoustooptical mode converter has been measured by scanning the surface of the sample with a focused HeNe laser beam and detecting the optical power diffracted by the SAW-induced grating ("laser probing" [18]). The result of this measurement is shown in Fig. 5.
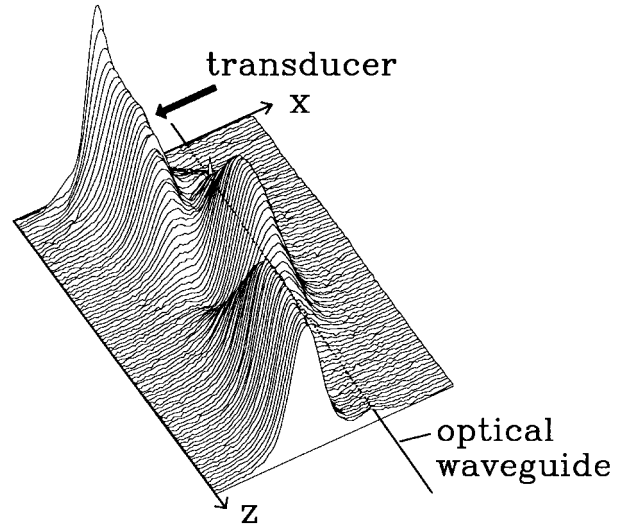

Fig. 5. SAW intensity distribution in the acoustooptical mode converter measured by laser probing.

The two couplers of the acoustooptic switch are laterally separated by a 170-μm-wide Ti-diffused area to achieve acoustical isolation. It has been measured indirectly by driving only one transducer at the power level necessary to achieve optimum conversion efficiency in the corresponding acoustooptical mode converter and measuring the conversion efficiency in the other mode converter (which should be zero in case of ideal acoustical isolation). The unwanted mode conversion has been measured to be below 1%. The optical power converted by the "wrong" SAW suffers a frequency-shift into opposite direction resulting in beating at twice the SAW frequency. However, the beating signal was too low to be measured; it was hidden in the noise of the pin-FET receiver used for detection.

The SAW's are excited via interdigital transducer electrodes (500-nm-thick aluminum) consisting of 20 finger pairs with a period of 20.8 μm. To absorb the acoustical power behind the transducer and at the end of the interaction length absorbers of UV-curing glue have been deposited.

E. Fiber-Chip Coupling

To reduce coupling losses between standard single-mode fibers and the optical waveguides the mode field distributions should be well matched. The depth profile of 7-μm-wide optical waveguide modes is stronger confined (FWHM of intensity distribution 4.3 μm for TM and 3.5 μm for TE) than that of the fiber (6.0 μm) resulting in coupling losses typically larger than 1 dB. To increase the waveguide mode sizes we use a linear taper of the waveguide width which is reduced to 5 μm. Theoretical coupling losses are below 0.5 dB; practically, the losses have been kept below 1 dB.

The endfaces of the sample have been polished and $\lambda/4$-layers made of Y_2O_3 ($n \approx 1.7$) have been deposited as antireflective coatings. To define the fiber's pitch they have been fixed in V-grooves fabricated by preferential etching in the surface of Silicon. Finally, the fibers have been glued to the optical waveguides using UV curing adhesive.
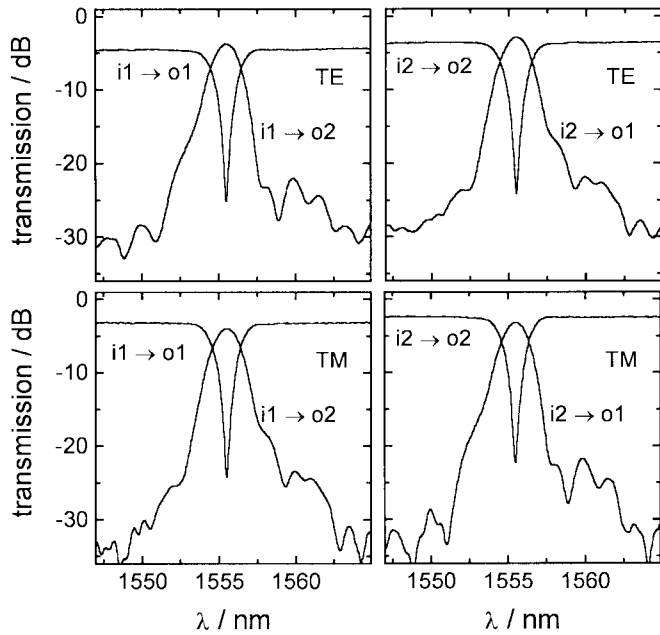
Fig. 6. Switching characteristics of the 2 × 2 switch. The diagrams show the transmission for TE and TM input polarization versus optical wavelength into the cross- and bar-states for both input ports.

Fig. 7. Switching characteristics of the 2 × 2 switch for both input ports at 45° linear input polarization.

F. Packaging

The 65-mm-long sample has been mounted on a copper block, which can be temperature stabilized using thermoelectric coolers. The switch is enclosed in an aluminum housing (80 × 120 × 40 mm^3) which also contains the electronic circuit to match the impedance of the transducer electrodes.

IV. DEVICE PERFORMANCE

The devices have been investigated measuring the transmission of the broad-band amplified spontaneous emission (ASE) of an erbium doped fiber amplifier with an optical spectrum analyzer (OSA) at a resolution of 0.1 nm. The ASE signal has been polarized using a fiber polarization splitter. The SAW frequency has been adjusted to yield polarization conversion and thereby switching at $\lambda = 1556$ nm. The results of these measurements are shown in Fig. 6. The 3-dB bandwidth is 2.0 nm. In the cross-state transmission spectra (i1→o2,i2→o1) sidelobes about −18.5 dB below the maximum level occur at the longer wavelength side that are mainly due to inhomogeneities of the optical waveguides [19], [20].

The transmission spectra i1→o2 (TE input, upper left diagram) and i2→o1 (TM input, lower right diagram) are quite similar. This is due to the fact that TE polarized waves entering input port i1 are routed to the same mode converter as TM polarized waves entering input port i2. Therefore, both spectra show the conversion characteristic of the lower mode converter (see Fig. 1). Analogous, the transmission spectra i1→o2 (TM input, lower left diagram) and i2→o1 (TE input, upper right diagram) resemble as well because both show the conversion characteristic of the upper mode converter. It is obvious, that the signal floor is higher in the upper diagrams than in the lower ones. This is a result of the polarization dependent splitting ratio of the polarization splitters. In case of the
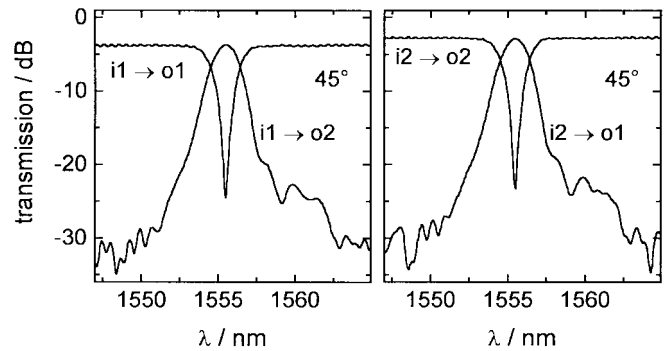
particular device reported here, the splitting ratio is 23 dB for TE and 33 dB for TM polarization.

The transmission spectra into the bar-state show a rejection of −20-dB worst case at $\lambda = 1556$ nm. This figure is limited by the splitting ratio of the polarization splitters and by the conversion efficiency of the acoustooptical mode converters. A crosstalk figure of −20 dB requires a conversion efficiency of 99%.

It is worth to notice that even the spectral transmission curves at 45° input polarization which are shown in Fig. 7 yield a bar-state rejection of better than −20 dB for both input ports. This can only be achieved if the rejection bands of both acoustooptical mode converters perfectly overlap. An input signal being unpolarized or polarized at 45° is launched to both acoustooptical mode converters by the first polarization splitter so that each converter contributes with 50% to the overall mode conversion. If the center wavelengths of the transmission curves corresponding to TE and TM input polarization are shifted against each other by $\Delta\lambda$, especially the rejection of the notch filter curve in the bar-state output decreases. If, e.g., the rejection is about −20 dB for TE and TM input, it decreases to −17 to −18 dB if $\Delta\lambda = 0.1$–0.2 nm.

The problem is, that (as already mentioned above) both mode converters have to be operated at the same RF frequency to avoid beating effects. This frequency, together with the wavelength dependent birefringence $\Delta\beta$ of the optical waveguides, defines the wavelength of maximum conversion efficiency in (1). Due to technological tolerances $\Delta\beta$ can be slightly different for the optical waveguides embedded in the two acoustooptical mode converters. This results in different wavelengths of maximum conversion efficiency.

Obviously, this problem can be solved by using acoustooptical mode converters with flat-top conversion characteristics [5]. For the device reported here $\Delta\lambda \approx 0$ has been observed resulting in strong rejection bands even at 45° input polarization. In a WDM system, the crosstalk from neighboring wavelengths depends on the wavelength channel separation. For a separation of 4 nm the inter-channel crosstalk is below −19.2 dB.

At 45° input polarization a modulation has been observed in the bar-state transmission spectra (see Fig. 7). This modulation is also present if the RF drive power is switched off. It can be explained by the polarization dependence of the OSA used
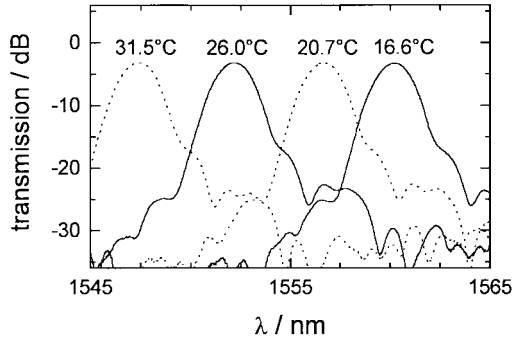
Fig. 8. Temperature dependence of the transmission characteristics. The device has been driven with a frequency of 174.5 MHz.
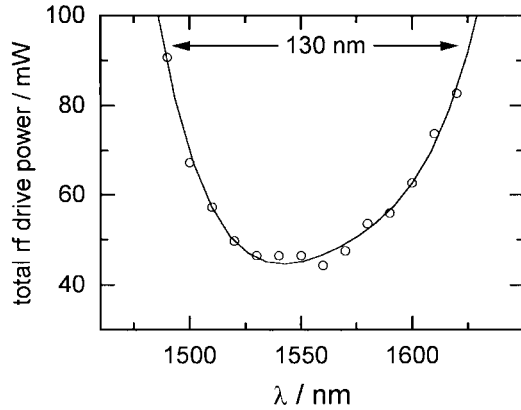

Fig. 9. Total RF drive power versus switching wavelength.

TABLE I
INSERTION LOSS IN DECIBELS (INCLUDING ONE FC/PC CONNECTION)

input port	i1		i2	
polarisation state	TE	TM	TE	TM
output port o1	4.6	3.3	3.0	3.1
output port o2	3.9	3.8	3.3	2.3

for the measurements in combination with the birefringence of LiNbO₃. The TM polarized waves are retarded with respect to the TE polarized waves when passing the device. After recombination in the output port the optical power is launched to the OSA that acts as a partial polarizer. The resulting interference leads to the observed modulation.

The fiber-to-fiber insertion loss of the switch can be derived from Fig. 6 but it has been measured with better accuracy at $\lambda = 1556$ nm using a DFB laser diode and an optical power meter which is not polarization dependent in contrast to the OSA used for the measurements shown in Fig. 6. The insertion loss is dependent on input port, input polarization, and switch state (see Table I).

The loss varies between 2.3 and 4.6 dB. The polarization dependence is 1.3 dB in the bar-state and only 0.1 dB in the cross-state. This is understandable as the main contributions to the insertion loss come from bending losses and fiber-chip-coupling losses and both are stronger for TE than for TM polarized waves. In bar-state operation the SOP does not change whereas for cross-state routing the SOP changes; half
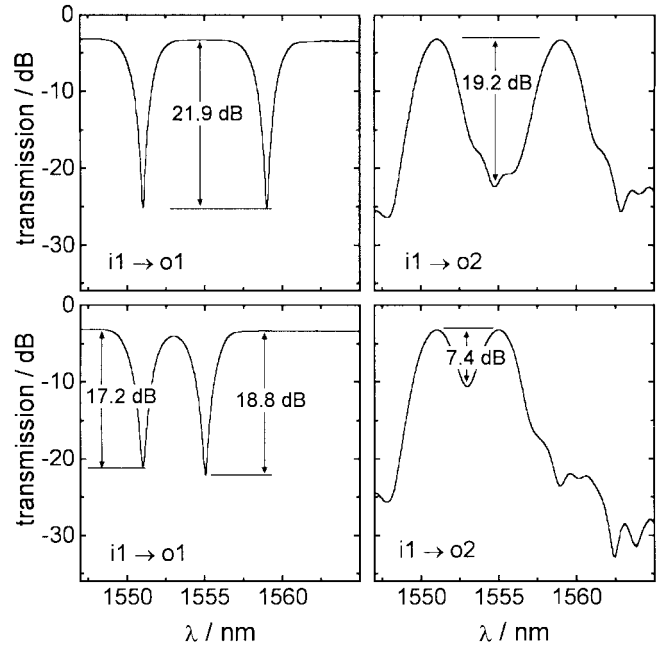

Fig. 10. Simultaneous two-wavelength operation. If the channels are 8 nm apart no perturbation is observed whereas the channels obviously affect each other in case of 4-nm channel spacing.

of the device is passed in TE polarization and the other half in TM. Thus, in the cross-state the average loss is independent of the input polarization.

In Fig. 8, the temperature dependence of the transmission characteristics is shown. The slope is given by $\partial\lambda/\partial T = -0.86$ nm/K. Therefore, to guarantee a wavelength stability of ±0.1 nm a temperature stabilization of ±0.12 K is necessary. Experimentally, the temperature of the copper block the sample is mounted on has been stabilised to ±0.02 K.

Tuning of the switch is achieved by varying the acoustic frequency; the tuning slope is given by -124 kHz/nm. The tuning range is mainly determined by the bandwidth of the transducers. In Fig. 9, the total electrical RF power required to drive the switch (i.e., to excite both transducers) is plotted versus the optical wavelength. The minimum drive power of 44 mW is required at $\lambda = 1560$ nm. The tuning range of 130 nm extends from 1490 to 1620 nm, defined by the wavelength range in which the drive power is below twice the minimum value.

To demonstrate the multiwavelength switching capability of the device it has been driven with two RF signals simultaneously switching two wavelengths 4 and 8 nm apart. In Fig. 10, the spectral dependencies of the transmission into the cross- and bar-states are shown for input i1 and TM input polarization. In the upper diagrams, a wavelength channel spacing of 8 nm was chosen. In this case, an extinction ratio of 21.9 dB is achieved in the bar-state output and the minimum between the transmission maxima of the cross-state output is 19.2 dB below the maximum value. When reducing the channel spacing to 4 nm (lower diagrams) the extinction ratio in the bar-state output decreases due to interchannel interaction [10], [22] and the cross-state output transmission spectrum shows a significant overlap of the transmission spectra of both channels.

V. Conclusion

We have developed and investigated integrated acoustooptic switches/add–drop multiplexers in LiNbO$_3$. The devices have been fully packaged and fiber pigtailed. An insertion loss of 4.6 dB and a residual polarization dependence of 1.3 dB in the worst case has been achieved. The sidelobe suppression has been measured to be better than -18 dB, the rejection of the bar-state transmission spectra is -20-dB worst case. The tuning range extends from 1490 to 1620 nm; at $\lambda = 1560$ nm an electrical drive power of only 44 mW is required.

Two devices have been successfully demonstrated at the European Exhibition on Optical Communication 1995 (EEOC'95) where they have been part of two OADM nodes in a self-healing ring similar to that described in [21] which was developed within the EU-RACE project "MWTN" (Multi-Wavelength Transport Network). The OADM nodes have also been investigated within the Stockholm Gigabit Network and the East Anglian Network testbed. Further devices are currently investigated in testbeds of the Research Institute of the German Telekom.

The performance of the switches can be further improved by implementation of acoustooptical mode converters witch flat-top conversion characteristics [5]. This will make the devices less sensitive to fabrication tolerances as well as temperature and laser wavelength drifts. However, the device lengths as well as sidelobes increase if the transmission characteristics is flattened. To get a 2×2 switch matrix/add–drop multiplexer with improved crosstalk figures one can also make use of dilation, i.e., cascading the devices [11]. This results in increased insertion losses which is a clear disadvantage as well.

References

[1] K. W. Cheung, "Acoustooptic tunable filters in narrowband WDM networks: system issues and network applications," *IEEE J. Select. Areas Commun.*, vol. 8, pp. 1015–1025, 1990.
[2] G. R. Hill *et al.*, "A transport network layer based on optical network elements," *J. Lightwave Technol.*, vol. 11, pp. 667–679, 1993.
[3] H. Herrmann, D. A. Smith, and W. Sohler, "Integrated optical, acoustically tunable wavelength filters and switches and their network applications," in *Proc. Eur. Conf. Integrated Optics (ECIO'93)*, Neuchâtel, Switzerland, pp. 10-1–10-3, 1993.
[4] F. Tian, Ch. Harizi, H. Herrmann, V. Reimann, R. Ricken, U. Rust, W. Sohler, F. Wehrmann, S. Westenhöfer, "Polarization-independent integrated optical, acoustically tunable double-stage wavelength filter in LiNbO$_3$," *J. Lightwave Technol.*, vol. 12, no. 7, pp. 1192–1197, 1994.
[5] J. L. Jackel, J. E. Baran, A. d'Alessandro, and D. A. Smith, "A passband-flattened acousto-optic filter," *IEEE Photon. Technol. Lett.*, vol. 7, pp. 318–320, Mar. 1995.
[6] A. d'Alessandro, D.A. Smith, and J.E. Baran, "Multichannel operation of an integrated acousto-optic wavelength routing switch for WDM systems," *IEEE Photon. Technol. Lett.*, vol. 6, pp. 390–393, Mar. 1995.
[7] F. Wehrmann, Ch. Harizi, H. Herrmann, U. Rust, W. Sohler, S. Westenhöfer, "Fully packaged, integrated optical, acoustically tunable add-drop multiplexers in LiNbO$_3$," in *Eur. Conf. Integrated Optics, ECIO'95*, Delft, The Netherlands, 1995, pp. 487–490.
[8] W. I. Way, D. A. Smith, J. J. Johnson, and H. Izadpanah, "A self-routing WDM high-capacity SONET ring network," *IEEE Photon. Technol. Lett.*, vol. 4, pp. 402–405, Apr. 1992.
[9] D. A. Smith and J. J. Johnson, "Sidelobe suppression in an acousto-optic filter with a raised-cosine interaction strength," *Appl. Phys. Lett.*, vol. 61, pp. 1025–1027, 1992.
[10] J. L. Jackel, J. E. Baran, G.-K. Chang, M. Z. Iqbal, G. Hugh Song, W. J. Tomlinson, D. Fritz, and R. Ade, "Multichannel operation of AOTF switches: reducing channel-to-channel interaction," *IEEE Photon. Technol. Lett.*, vol. 7, pp. 370–372, Apr. 1995.
[11] D. A. Smith, A. d'Alessandro, J. E. Baran, D. J. Fritz, and R. H. Hobbs, "Reduction of cross talk in an acousto-optic switch by means of dilation," *Opt. Lett.*, vol. 19, no. 2, pp. 99–101, 1994.
[12] H. Herrmann, U. Rust, and K. Schäfer, "Tapered acoustical directional couplers for integrated acousto-optic mode converters with weighted coupling," *J. Lightwave Technol.*, vol. 13, pp. 364–374, Mar. 1995.
[13] L. B. Aronson, G. Rankin, W. R. Trutna, Jr., and D. W. Dolfi, "Reduced sidelobe integrated acousto-optic filter with birefringence apodization," *Opt. Lett.*, vol. 18, no. 20, pp. 1721–1723, 1993.
[14] H. Herrmann and St. Schmid, "Integrated acousto-optic mode-convertors with weighted coupling using surface acoustic wave directional couplers," *Electron. Lett.*, vol. 28, no. 11, pp. 979–980, 1992.
[15] Y. Yamamoto, C.S. Tsai, K. Esteghamat, and H. Nishimoto, "Suppression of sidelobe levels for guided-wave acousto-optic tunable filters using weighted coupling," *IEEE Trans. Ultrason., Ferroelec., Frequency Contr.*, vol. 40, pp. 814–818, Nov. 1993.
[16] A. Kar-Roy and Ch. S. Tsai, "Ultralow sidelobe-level integrated acoustooptic tunable filters using tapered-gap surface acoustic wave directional couplers," *J. Lightwave Technol.*, vol. 12, 1994.
[17] A. Kar-Roy and Ch.S. Tsai, "Integrated acoustooptic tunable filters using weighted coupling," *IEEE J. Quantum Electron.*, vol. 30, pp. 1574–1586, July 1994.
[18] E. G. H. Lean and C. G. Powell, "Optical probing of surface acoustic waves," *Proc. IEEE*, vol. 58, pp. 1939–1947, 1970.
[19] D. A. Smith, A. d'Alessandro, J. E. Baran, and H. Herrmann, "Source of sidelobe asymmetry in acousto-optic tunable filters," *Appl. Phys. Lett.*, vol. 62, pp. 814–816, 1993
[20] W. R. Trutna, Jr., D. W. Dolfi, and C. A. Flory, "Anomalous sidelobes and birefringence apodization in acousto-optic tunable filters," *Opt. Lett.*, vol. 18, no. 1, pp. 28–30, 1993
[21] E. Almström, Ch. Hübinette, Å. Karlsson, and S. Johansson, "A unidirectional self-healing ring using WDM technique," in *Proc. Eur. Conf. Optical Communication (ECOC'94)*, Firenze, Italy, 1994, vol. 2, pp. 873–875.
[22] F. Tian and H. Herrmann, "Interchannel Interference in Multiwavelength Operation of Integrated Acousto-Optical Filters and Switches," *J. Lightwave Technol.*, vol. 13, pp. 1146–1154, June 1995.

Frank Wehrmann studied physics at the University of Hamburg/Germany in cooperation with the Technical University of Hamburg-Harburg, Department of Electrical Engineering and received the diploma degree in 1991.

Since 1992, he is with the University of Paderborn/Germany, Department of Applied Physics, working on integrated acoustooptical filters and switches.

Mr. Wehrmann is a member of the German Physical Society.

Christiane Harizi studied physics at the University of Paderborn and received the Diplom-Physikingenieur degree in 1992.

She then joined the Department of Applied Physics of the University of Paderborn working on technology and fabrication of integrated optical circuits in lithium niobate.

Harald Herrmann received the diploma degree in physics from the University of Hannover in 1984 and the Ph.D. degree (Dr. rer. nat.) with a thesis on nonlinear difference frequency generation in lithium niobate waveguides from University of Paderborn, Germany in 1991.

In 1984, he joined the Department of Applied Physics of the University of Paderborn, Germany. There he was engaged in the development of color center lasers and in investigations of nonlinear processes in integrated optical waveguides and new electrooptical an acoustooptical devices. He currently works on integrated acoustooptical devices and their applications in optical communication systems and optical instrumentation.

Dr. Herrmann is a member of the German Physical Society.

Ulrich Rust (S'94) studied physics at the University of Edinburgh, U.K. and the University of Paderborn, where he received the Diplom-Physiker degree in 1992.

Since then he has been working on numerical simulations of integrated acoustooptical devices in lithium niobate in the Department of Applied Physics.

Mr. Rust is a member of the German Physical Society.

Susanne Westenhöfer first served an apprenticeship as photographer and then studied photoengineering in Cologne, Germany, with main focus on technical optics and interferometry. She received the B.E. degree in 1991.

She joined the University of Paderborn in 1992, working in research on optical guided wave devices, particularly in chip-to-fiber attachment. Since 1996, she is with the Paul Scherrer Institute, Zurich, Switzerland.

Wolfgang Sohler received the Diplom-Physiker and Dr. rer. nat. degrees in physics from the University of Munich, Germany, in 1970 and 1974, respectively.

From 1975 to 1980, he was with the University of Dortmund/Germany working on integrated optics. In 1980, he joined the Fraunhofer Institut für Physikalische Meßtechnik, Freiburg, Germany, as head of the Department of Fiber Optics. Since 1982, he is with the University of Paderborn/Germany, as Professor of Applied Physics. His research interests include integrated optics, fiber optics and laser physics. He is the (co-)author of more than 100 journal contributions and of several book chapters. He has been a member of the program committee of several (international) conferences on integrated optics.

Dr. Sohler is a member of the German Physical Society and of the German Society of Applied Optics.